

Iterative global-local approach to consider the local effects in dynamic analysis of beams

R. Emre Erkmen* and Ashkan Afnani^a

*School of Civil and Environmental Engineering, University of Technology, Sydney,
15 Broadway, Ultimo NSW 2007, Australia*

(Received November 9, 2016, Revised November 13, 2017, Accepted November 14, 2017)

Abstract. This paper introduces a numerical procedure to incorporate elasto-plastic local deformation effects in the dynamic analysis of beams. The appealing feature is that simple beam type finite elements can be used for the global model which needs not to be altered by the localized elasto-plastic deformations. An overlapping local sophisticated 2D membrane model replaces the internal forces of the beam elements in the predefined region where the localized deformations take place. An iterative coupling technique is used to perform this replacement. Comparisons with full membrane analysis are provided in order to illustrate the accuracy and efficiency of the method developed herein. In this study, the membrane formulation is able to capture the elasto-plastic material behaviour based on the von Mises yield criterion and the associated flow rule for plane stress. The Newmark time integration method is adopted for the step-by-step dynamic analysis.

Keywords: iterative global-local method; multi-scale analysis; finite elements; elasto-plastic behavior; structural dynamics

1. Introduction

There is a need for computationally efficient structural dynamic analysis methods to gain savings in analysis time as well as in the post-processing of the results, despite significant advances in computer performances. It is possible to improve the accuracy of the numerical results by refining the model only in a local region without changing the global simpler model of the whole structure (Knight *et al.* 1991, Mao and Sun 1991, Mote 1971, Noor 1986). Simple beam elements are often used in the modelling of frame type structures, such as buildings or bridges, since frame-type structures are composed of beams and columns that have one dimension relatively large in comparison to the cross-sectional dimensions. Simple beam-type elements, however, are based on the assumption of rigid cross-section and thus, they cannot consider the deformations of the cross-section. On the other hand, local effects in beams may interact with the global behaviour to produce early yielding and reduction in strength. Overlapping decomposition

*Corresponding author, Ph.D., E-mail: emre.erkmen@uts.edu.au

^aPh.D., E-mail: ashkan.afnani@student.uts.edu.au

of the analysis domain allows a local enrichment which can seamlessly incorporate local deformation effects as used in various types of problems (Babuska and Melenk 1995, Belytschko 2001, Belytschko *et al.* 1996, Duarte and Oden 1996, Duval *et al.* 2016, Erkmen and Bradford 2011, Erkmen 2013, Erkmen 2015, Feyerl 2003, Fish *et al.* 1994, Hughes *et al.* 1998, Hughes and Sangalli 2007, Liu *et al.* 2000, Strouboulis *et al.* 2001).

In particular, global-local technique has been employed by Doyle and his colleagues for the dynamic analysis of damaged structures (Doyle and Farris 1995, Farris and Doyle 1993) in order to determine stress intensity factors around the cracked regions in damaged beams. However, they did not consider the effects of local deformations on the global behaviour, which requires iterative global-local approaches (Mao and Sun 1991, Whitcomb and Woo 1993a, Whitcomb 1991). By using iterative global-local approaches the same level of accuracy, which can be obtained from the fully fine mesh solution, can be retained (Bettinotti *et al.* 2014, Gendre *et al.* 2009, Kerfriden *et al.* 2012, Mao and Sun 1991, Voletti 1996, Whitcomb and Woo 1993a, Whitcomb 1993b). These approaches have been applied for static analysis in various different contexts by Whitcomb and his colleagues (Whitcomb 1991, Whitcomb and Woo 1993a, 1993b) and by Sun and Mao (1988). Recently, similar approaches have been applied to capture local buckling effects in steel and composite structural elements by Afnani and Erkmen (2016), Erkmen *et al.* (2016), Erkmen and Saleh (2017) and Erkmen *et al.* (2017).

In dynamic analysis of structures such as seismic performance evaluation (Lim *et al.* 2016, Bozdogan and Ozturk 2016) or wind (Banik *et al.* 2010), blast and impact load analyses (Hadianfard *et al.* 2012, McConnell and Brown 2011), it is often important to consider local nonlinearities that occur in the behaviour. With this motivation in mind, an iterative global-local analysis technique is introduced herein for nonlinear dynamic analysis of structures. We illustrate that the proposed technique is efficient when complex structures that contain small nonlinear areas are analysed. A beam element is used as the global model while a 2D membrane finite element with elasto-plastic formulation is adopted as the local model. In each analysis iteration, the internal stress field in the membrane element is compared against the stress resultants of the global model, and the difference is corrected by applying additional unbalanced forces to the global model until convergence is achieved. The Newmark time integration method is adopted for the step-by-step dynamic analysis. The closest-point projection algorithm along with the consistent tangent modulus is adopted for the elasto-plastic plane-stress calculations of the local membrane model. Throughout the analysis, local nonlinearities are contained in the local membrane model which does not require modifications in the global model; hence the method is considered as non-intrusive (e.g., Allix *et al.* 2011).

The paper is organised as follows; the beam formulation is introduced in Section 2. A local membrane finite element model is introduced in Section 3. Both beam and membrane formulations are standard and only briefly explained. Coupled global-local equilibrium equations, their linearization and the interface boundary conditions between the beam and membrane models are also discussed in Section 3. Elasto-plastic constitutive equations and the stress update algorithm for the local membrane model are given in Section 4. The equilibrium equations of the global-local approach are obtained in Section 5. These equations are solved iteratively based on the Newmark's step-by-step time integration strategy as also briefly explained in Section 5. Numerical examples are presented in Section 6 and conclusions are drawn in Section 7.

2. Beam element formulation with local enrichment

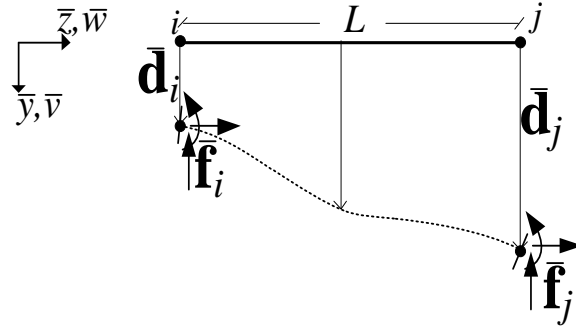


Fig. 1 Forces and displacements at the ends of the beam

2.1 Kinematic description

A beam element, based on the Euler-Bernoulli beam theory, is used for the global analysis of the structure. The formulation of this element is based on the three assumptions, which are: (a) beam axis stays perpendicular to the cross-section after deformations; (b) cross-sectional plane remains rigid throughout deformations; (c) normal stresses perpendicular to the axis line of the member are assumed to be zero. As shown in Fig. 1, vectors $\bar{\mathbf{d}}$ and $\bar{\mathbf{f}}$ are the end displacements and end forces of the beam before the local effects are considered. This initial configuration can be thought of as a trial state before the final configuration.

2.2 Strains

Strain components of the beam formulation can be written in terms of deflections $\bar{v}(\bar{z})$ and $\bar{w}(\bar{z})$, which are parallel to \bar{y} and \bar{z} directions, respectively as shown in Fig. 1. The generalized displacement field of a point on the cross-section is $\bar{\mathbf{u}} = \langle \bar{w}_p \quad \bar{v}_p \quad \bar{\theta}_p \rangle^T$ where $\bar{\mathbf{u}} = \mathbf{N}\bar{\mathbf{d}}$, in which \mathbf{N} is the matrix of interpolation functions and $\bar{\mathbf{d}}$ is the vector of nodal displacements. Matrix \mathbf{N} can be written as $\mathbf{N} = \mathbf{Y}\mathbf{Z}$ in which

$$\mathbf{Z} = \begin{bmatrix} \mathbf{L}^T & \mathbf{0} \\ \mathbf{0} & \mathbf{H}^T \\ \mathbf{0} & \frac{d\mathbf{H}^T}{d\bar{z}} \end{bmatrix}, \tag{1}$$

and

$$\mathbf{Y} = \begin{bmatrix} 1 & 0 & -\bar{y} \\ 0 & 1 & 0 \end{bmatrix}, \tag{2}$$

in which

$$\mathbf{L} = \left\langle 1 - \frac{\bar{z}}{L} \quad \frac{\bar{z}}{L} \right\rangle^T, \quad (3)$$

and

$$\mathbf{H} = \left\langle 1 - \frac{3\bar{z}^2}{L^2} + \frac{2\bar{z}^3}{L^3} \quad \bar{z} - \frac{2\bar{z}^2}{L} + \frac{\bar{z}^3}{L^2} \quad \frac{3\bar{z}^2}{L^2} - \frac{2\bar{z}^3}{L^3} \quad -\frac{\bar{z}^2}{L} + \frac{\bar{z}^3}{L^2} \right\rangle^T. \quad (4)$$

The nodal displacement vector $\bar{\mathbf{d}}$ of the beam-type finite element can be written as

$$\bar{\mathbf{d}} = \left\langle \bar{w}_1 \quad \bar{w}_2 \quad \bar{v}_1 \quad \bar{\theta}_{x1} \quad \bar{v}_2 \quad \bar{\theta}_{x2} \right\rangle^T, \quad (5)$$

in which subscripts 1 and 2 refer to each of the two end nodes and $\bar{\theta}_x$ refer to bending rotations in \bar{z} - \bar{y} plane. The strain field of a point on the cross-section can be written as

$$\boldsymbol{\varepsilon} = \mathbf{S}\bar{\boldsymbol{\chi}} = \langle \bar{\varepsilon} \quad 0 \quad 0 \quad 0 \rangle^T \quad (6)$$

which can be decomposed in terms of a matrix of cross-sectional coordinates, i.e.,

$$\mathbf{S} = \begin{bmatrix} 1 & 0 & 0 & 0 \\ \bar{y} & 0 & 0 & 0 \end{bmatrix}^T \quad (7)$$

and a vector of linear displacement derivatives, i.e.,

$$\bar{\boldsymbol{\chi}} = \langle \bar{w}' \quad \bar{v}'' \rangle^T. \quad (8)$$

In Eq. (8), prime denotes derivative with respect to the axial coordinate z , i.e., $(\prime) = d(\prime)/dz$ and in Eq. (7), \bar{y} identifies coordinates of a point on the cross-section. It should be noted that although the strain in the Euler-Bernoulli beam theory is single-dimensional, the organization of Eq. (6) is such that the beam strains and consequently stresses are comparable with those of the membrane's in Section 3.

2.3 Variational formulation

The variational form of equilibrium equations can be written as

$$\delta \bar{\Pi} = \int_L \int_A \delta \bar{\boldsymbol{\varepsilon}}^T \bar{\boldsymbol{\sigma}} dA d\bar{z} + \int_L \int_A \delta \bar{\mathbf{u}}^T \mathbf{c} \dot{\bar{\mathbf{u}}} dA d\bar{z} + \int_L \int_A \delta \bar{\mathbf{u}}^T \boldsymbol{\rho} \ddot{\bar{\mathbf{u}}} dA d\bar{z} - \delta \bar{\mathbf{d}}^T \bar{\mathbf{f}} = 0 \quad (9)$$

in which $\bar{\boldsymbol{\sigma}}$ is the stress in the beam element, A is the cross-sectional area, L is the beam span, \mathbf{c} is the damping matrix, $\dot{\bar{\mathbf{u}}}$ is the velocity vector, $\boldsymbol{\rho}$ is the material density matrix, and $\ddot{\bar{\mathbf{u}}}$ is the acceleration vector. The stress in Eq. (9) can be obtained directly from the strains using the linear stress-strain relationship for an isotropic material as the beam model is assumed elastic, i.e., $\bar{\boldsymbol{\sigma}} = \bar{\mathbf{E}}\bar{\boldsymbol{\varepsilon}}$ in which,

$$\bar{\mathbf{E}} = \begin{bmatrix} E & 0 & 0 & 0 \\ 0 & 0 & 0 & 0 \\ 0 & 0 & 0 & 0 \\ 0 & 0 & 0 & 0 \end{bmatrix} \quad (10)$$

The variation of the strain field of a point on the cross-section of the beam element can also be decomposed into two parts which can be written as

$$\delta \bar{\boldsymbol{\varepsilon}} = \mathbf{S} \bar{\mathbf{B}} \delta \bar{\mathbf{d}}, \quad (11)$$

in which expressions $\bar{\mathbf{B}}$ can be written as $\bar{\mathbf{B}} = \nabla \mathbf{X}_a$ where

$$\nabla = \begin{bmatrix} \frac{d}{dz} & 0 \\ 0 & \frac{d^2}{dz^2} \end{bmatrix} \quad (12)$$

and

$$\mathbf{X}_a = \begin{bmatrix} \mathbf{L}^T & \mathbf{0} \\ \mathbf{0} & \mathbf{H}^T \end{bmatrix}. \quad (13)$$

By substituting Eq. (11) into Eq. (9), one obtains

$$\delta \bar{\Pi} = \delta \bar{\mathbf{d}}^T \int_{L A} \bar{\mathbf{B}}^T \mathbf{S}^T \bar{\boldsymbol{\sigma}} dA d\bar{z} + \delta \bar{\mathbf{d}}^T \int_{L A} \mathbf{N}^T \mathbf{c} \dot{\bar{\mathbf{d}}} dA d\bar{z} + \delta \bar{\mathbf{d}}^T \int_{L A} \mathbf{N}^T \rho \ddot{\bar{\mathbf{d}}} dA d\bar{z} - \delta \bar{\mathbf{d}}^T \bar{\mathbf{f}} = 0. \quad (14)$$

2.4 Linearization of the dynamic equilibrium equations

The incremental equilibrium equations can be obtained by subtracting the virtual work expressions in Eq. (14) at two neighbouring equilibrium states and then linearizing the result by omitting the second- and higher-order terms, i.e.,

$$\delta(\delta \bar{\Pi}) \approx \delta \bar{\mathbf{d}}^T \bar{\mathbf{K}} \delta \bar{\mathbf{d}} + \delta \bar{\mathbf{d}}^T \bar{\mathbf{C}} \dot{\delta \bar{\mathbf{d}}} + \delta \bar{\mathbf{d}}^T \bar{\mathbf{M}} \ddot{\delta \bar{\mathbf{d}}} - \delta \bar{\mathbf{d}}^T \delta \bar{\mathbf{f}} = 0, \quad (15)$$

where

$$\bar{\mathbf{K}} = \int_{L A} \bar{\mathbf{B}}^T \mathbf{S}^T \bar{\mathbf{E}} \mathbf{S} \bar{\mathbf{B}} dA d\bar{z}, \quad (16)$$

$$\bar{\mathbf{C}} = \int_{L A} \mathbf{N}^T \mathbf{c} \mathbf{N} dA d\bar{z} \quad (17)$$

and

$$\bar{\mathbf{M}} = \int_L \int_A \mathbf{N}^T \boldsymbol{\rho} \mathbf{N} dA d\bar{z} \quad (18)$$

3. Local membrane solution

The membrane element used is a four-node, three-degree-of-freedom-per-node element based on the element developed by Ibrahimbegovic *et al.* (1990), which employs the drilling degree of freedom. Strains of the membrane element can be expressed in terms of drilling rotation $\hat{\theta}$ around x direction, and deflections \hat{u}_0 and \hat{v}_0 of the mid-surface in y - z plane. The Allman-type interpolation functions are used for membrane displacements \hat{u}_0 and \hat{v}_0 while standard bilinear interpolations are adopted for the drilling degree of freedom $\hat{\theta}$.

3.1 Variational formulation of the equilibrium equations and linearization

The variational form of the equilibrium equation of the membrane element can be written as

$$\delta \hat{\Pi} = \int_L \int_A \delta \hat{\boldsymbol{\varepsilon}}^T \hat{\boldsymbol{\sigma}} dA d\bar{z} + \int_L \int_A \delta \hat{\mathbf{u}}^T \hat{\mathbf{c}} dA d\bar{z} + \int_L \int_A \delta \hat{\mathbf{u}}^T \hat{\boldsymbol{\rho}} \hat{\mathbf{u}} dA d\bar{z} - \delta \hat{\mathbf{d}}^T \hat{\mathbf{f}} = 0, \quad (19)$$

where $\hat{\boldsymbol{\varepsilon}}$ is the strain vector of the membrane element, which is expressed explicitly in Appendix A. It should be noted that, the strain vector $\bar{\boldsymbol{\varepsilon}}$ of the beam formulation can be obtained by substituting the displacement field $\bar{\mathbf{u}}$ (which imposes beam kinematics) into membrane strain expressions $\hat{\boldsymbol{\varepsilon}}$ as given in Appendix A. It should also be noted that the virtual work expression of the membrane element is modified in order to avoid numerical stability issues with Allman type interpolations of the membrane component as suggested in Ibrahimbegovic *et al.* (1990) and thus, the skew symmetric part of the membrane strains and associated drilling rotations are contained in the first term in Eq. (19). The local membrane behaviour is assumed elasto-plastic. Therefore, a numerical procedure is required to obtain the stress field $\hat{\boldsymbol{\sigma}}$. The details of the numerical procedure are given in section 4. In the last term of Eq. (19), $\hat{\mathbf{f}}$ is the external load vector and $\hat{\mathbf{d}}$ is the vector of nodal displacements.

The first variation of the strain vector used in Eq. (19) can be expressed as

$$\delta \hat{\boldsymbol{\varepsilon}} = \hat{\mathbf{B}} \delta \hat{\mathbf{d}}, \quad (20)$$

where $\hat{\mathbf{B}}$ and $\hat{\mathbf{d}}$ are presented explicitly in Appendix A. In order to obtain the incremental equilibrium equations of the membrane analysis, the weak form of the equilibrium equations in Eq. (19) has to be derived and subtracted at two neighbouring equilibrium states. Linearizing the results, i.e., omitting the second- and higher-order terms, gives rise to

$$\delta(\delta \hat{\Pi}) \approx \delta \hat{\mathbf{d}}^T \hat{\mathbf{K}} \delta \hat{\mathbf{d}} + \delta \hat{\mathbf{d}}^T \hat{\mathbf{C}} \delta \hat{\mathbf{d}} + \delta \hat{\mathbf{d}}^T \hat{\mathbf{M}} \delta \hat{\mathbf{d}} - \delta \hat{\mathbf{d}}^T \delta \hat{\mathbf{f}} = 0, \quad (21)$$

$\hat{\mathbf{K}}$ in Eq. (21) is the stiffness matrix of the membrane model, i.e.,

$$\hat{\mathbf{K}} = \int \int_{L A} \hat{\mathbf{B}}^T \hat{\mathbf{C}}_{ep} \hat{\mathbf{B}} dA d\bar{z}, \quad (22)$$

where $\hat{\mathbf{C}}_{ep}$ is the elasto-plastic stress-strain matrix as explained in section 4.1. and

$$\hat{\mathbf{C}} = \int \int_{L A} \hat{\mathbf{X}}^T \mathbf{c} \hat{\mathbf{X}} dA d\bar{z} \quad (23)$$

$$\hat{\mathbf{M}} = \int \int_{L A} \hat{\mathbf{X}}^T \rho \hat{\mathbf{X}} dA d\bar{z} \quad (24)$$

where $\delta \hat{\mathbf{u}} = \hat{\mathbf{X}} \delta \hat{\mathbf{d}}$ was used.

3.2 Displacement decomposition

The membrane displacement vector is decomposed into two parts: a global component, which is in accordance with the kinematic assumption of the beam element, and a remaining part that is the difference between the total membrane displacements and the global component. To build the global component, a decomposition operator is adopted that projects the nodal displacement of the beam onto the nodal points of the membrane model, i.e., $\hat{\mathbf{d}} = \mathbf{N} \bar{\mathbf{d}} + \mathbf{d}'$, the variation of the membrane nodal displacement vector can be written as

$$\delta \hat{\mathbf{d}} = \mathbf{N} \delta \bar{\mathbf{d}} + \delta \mathbf{d}', \quad (25)$$

It should be noted that as opposed to its use in section 2.1, where it was imposing the kinematic conditions on a continuum, \mathbf{N} operates on discrete coordinates \bar{y} and \bar{z} of the local membrane model nodes. By adopting \mathbf{N} as the decomposition operator, it is assumed that outside of the overlapping region where \mathbf{d}' is a zero vector, the beam displacements are identical with those of the possible membrane solution.

3.3 Coupled global and local equilibrium equations

We can decompose the first variation of the membrane strain based on the abovementioned decomposition of the variation of the displacement vector $\delta \hat{\mathbf{d}}$ by substituting Eq. (25) into Eq. (20), i.e., $\delta \hat{\boldsymbol{\varepsilon}} = \delta \bar{\boldsymbol{\varepsilon}} + \delta \boldsymbol{\varepsilon}'$, where

$$\delta \bar{\boldsymbol{\varepsilon}} = \hat{\mathbf{B}} \mathbf{N} \delta \bar{\mathbf{d}}, \quad (26)$$

and

$$\delta \boldsymbol{\varepsilon}' = \hat{\mathbf{B}} \delta \mathbf{d}'. \quad (27)$$

As discussed previously, the first component of the membrane displacement is obtained by imposing beam kinematics on the membrane solution. Consequently, the variation of this component of the membrane strain vector is equal to that of the beam i.e., $\hat{\mathbf{B}} \mathbf{N} = \mathbf{S} \bar{\mathbf{B}}$. The second

term in the right-hand side of Eq. (25) i.e., $\delta\mathbf{d}'$, produces $\delta\boldsymbol{\varepsilon}'$, which describes the difference between the variations of the strain fields. By using Eqs. (26) and (27) in Eq. (19), the decomposed equilibrium equations can be obtained as

$$\delta\Pi_1 = \delta\bar{\mathbf{d}}^T \mathbf{N}^T \int \int_{L,A} \hat{\mathbf{B}}^T \hat{\boldsymbol{\sigma}} dAd\bar{z} + \delta\bar{\mathbf{d}}^T \mathbf{N}^T \hat{\mathbf{C}} \hat{\mathbf{d}} + \delta\bar{\mathbf{d}}^T \mathbf{N}^T \hat{\mathbf{M}} \hat{\ddot{\mathbf{d}}} - \delta\bar{\mathbf{d}}^T \mathbf{N}^T \hat{\mathbf{f}} = 0, \quad (28)$$

and

$$\delta\Pi_2 = \delta\mathbf{d}'^T \int \int_{L,A} \hat{\mathbf{B}}^T \hat{\boldsymbol{\sigma}} dAd\bar{z} + \delta\mathbf{d}'^T \hat{\mathbf{C}} \hat{\mathbf{d}} + \delta\mathbf{d}'^T \hat{\mathbf{M}} \hat{\ddot{\mathbf{d}}} - \delta\mathbf{d}'^T \mathbf{f} = 0, \quad (29)$$

It should be noted that in Eq. (28) the relation $\int \int_{L,A} \mathbf{N}^T \hat{\mathbf{B}}^T \hat{\boldsymbol{\sigma}} dAd\bar{z} = \mathbf{N}^T \int \int_{L,A} \hat{\mathbf{B}}^T \hat{\boldsymbol{\sigma}} dAd\bar{z}$ have been used as matrix \mathbf{N} is acting on the discrete nodal values. By considering a load case where $\mathbf{N}^T \hat{\mathbf{f}} = \bar{\mathbf{f}}$, and using the relations $\hat{\mathbf{B}}\mathbf{N} = \mathbf{S}\bar{\mathbf{B}}$, $\mathbf{N}^T \hat{\mathbf{C}}\mathbf{N} \approx \bar{\mathbf{C}}$ and $\mathbf{N}^T \hat{\mathbf{M}}\mathbf{N} \approx \bar{\mathbf{M}}$, Eq. (28) can be written as

$$\delta\Pi_1 = \delta\bar{\Pi} + \delta\bar{\mathbf{d}}^T \mathbf{F} = 0 \quad (30)$$

in which

$$\mathbf{F} = \mathbf{N}^T \int \int_{L,A} \hat{\mathbf{B}}^T \hat{\boldsymbol{\sigma}} dAd\bar{z} - \int \int_{L,A} \bar{\mathbf{B}}^T \mathbf{S}^T \bar{\boldsymbol{\sigma}} dAd\bar{z} \quad (31)$$

is a complementary force vector to consider the difference in the stresses of the local membrane and the beam models (Erkmen 2013). The difference between the beam equilibrium equations shown in Eq. (14) and Eq. (28) are the last two terms of Eq. (30).

3.4 Linearization of the coupled global-local equilibrium equations

By conveniently defining the difference in the local and global displacement fields as $\delta\mathbf{d}' = \mathbf{N}\delta\mathbf{c} + \mathbf{Q}_K\delta\mathbf{q}$, $\delta\mathbf{d}' = \mathbf{Q}_C\delta\dot{\mathbf{q}}$ and $\delta\mathbf{d}' = \mathbf{Q}_M\delta\ddot{\mathbf{q}}$, it can be shown that the linearization of Eq. (30) produces;

$$\delta(\delta\Pi_1) \approx \delta\bar{\mathbf{d}}^T \bar{\mathbf{K}} \delta\bar{\mathbf{d}} - \delta\bar{\mathbf{d}}^T \delta\bar{\mathbf{f}} = 0, \quad (32)$$

This can be verified by selecting \mathbf{Q}_K in $\delta\mathbf{d}'$ as

$$\mathbf{Q}_K = \mathbf{Q}_K - \mathbf{N} \left[\mathbf{N}^T \hat{\mathbf{K}} \mathbf{N} \right]^{-1} \mathbf{N}^T \hat{\mathbf{K}} \mathbf{Q}_K, \quad (33)$$

so that $\delta\mathbf{q}$ is arbitrary. The information carried between the beam model and the membrane model is linked through operator \mathbf{N} which is based on beam kinematics and the role of the operator \mathbf{Q}_K is to subtract the information that can be expressed by the beam model from the local membrane model solution. On the other hand, $\delta\mathbf{c}$ is introduced in $\delta\mathbf{d}'$ because of the differences due to separate constitutive matrices used in the beam and membrane models as well as the introduced discontinuities in the beam formulation that cannot be identified via operator \mathbf{Q}_K . Thus, $\delta\mathbf{c}$ can

be written as

$$\delta \mathbf{c} = - \left[\mathbf{N}^T \hat{\mathbf{K}} \mathbf{N} \right]^{-1} \left[\mathbf{N}^T \int_{L_A} \hat{\mathbf{B}}^T (\hat{\mathbf{C}}_{\mathcal{P}} - \bar{\mathbf{E}}) \hat{\mathbf{B}} dA d\mathcal{E} \mathbf{N} - \bar{\mathbf{K}} \right] \delta \bar{\mathbf{d}}, \quad (34)$$

It should also be noted that matrices \mathbf{Q}_C and \mathbf{Q}_M can be selected as

$$\mathbf{Q}_C = \mathbf{\Omega}_C - \mathbf{N} \left[\mathbf{N}^T \hat{\mathbf{C}} \mathbf{N} \right]^{-1} \mathbf{N}^T \hat{\mathbf{C}} \mathbf{\Omega}_C, \quad (35)$$

and

$$\mathbf{Q}_M = \mathbf{\Omega}_M - \mathbf{N} \left[\mathbf{N}^T \hat{\mathbf{M}} \mathbf{N} \right]^{-1} \mathbf{N}^T \hat{\mathbf{M}} \mathbf{\Omega}_M, \quad (36)$$

where $\mathbf{\Omega}_K$, $\mathbf{\Omega}_C$ and $\mathbf{\Omega}_M$ are time dependent matrix functions to build the relations $\delta \ddot{\mathbf{d}}' = \partial(\delta \dot{\mathbf{d}}') / \partial t = \partial^2(\delta \mathbf{d}') / \partial t^2$.

By linearization of Eq. (29) we have;

$$\delta(\delta \Pi_2) \approx \delta \mathbf{d}'^T \hat{\mathbf{K}} \delta \mathbf{d} - \delta \mathbf{d}'^T \delta \hat{\mathbf{f}} = 0. \quad (37)$$

It should be noted that the difference between Eqs. (21) and (37) is due to multiplication of the equations with $\delta \mathbf{d}'^T$ instead of $\delta \hat{\mathbf{d}}^T$. Considering the arbitrariness of both vectors, it can be concluded that both Eqs. (21) and (37) admit the same solution, which is the result of the membrane analysis for the whole domain of the structure. However, the solution of the beam model is deemed sufficiently accurate in regions that are not in the proximity of the localized behaviour where the local membrane solution is avoided for economy.

3.5 Interface boundary conditions

We obtain the local membrane solution within the overlapping domain by using the beam element displacement values as boundary conditions for the membrane model. It should be noted that the displacements of a point at the interface can be calculated only from the beam nodal displacements, i.e., $\mathbf{N}_{@i \& j} \bar{\mathbf{d}}$. Subscript $i \& j$ indicate both ends of the local membrane model. One important issue to be addressed before imposing the membrane boundary conditions is that even if there are no local effects, Poisson ratio effect causes change in the cross-sectional dimensions throughout the analysis domain. However, beam analysis does not produce a displacement field within the plane of the cross-section that captures the changes in cross-sectional dimensions due to Poisson ratio effect. On the other hand, this effect is considered in the stress field by adopting a separate constitutive relation in the beam formulation. Indeed, within the analysis region where beam solution is deemed accurate, we implicitly impose a strain field which can be considered within the current analysis framework as the Poisson ratio effect in the beam solution, i.e., $\boldsymbol{\varepsilon}' = \langle 0 \quad -\nu \varepsilon \quad 0 \quad 0 \rangle^T$, in which ε indicates the axial strain. It is important to note that this Poisson ratio effect has no influence on the beam equilibrium equations and the nodal displacement vector, because the associated stress field is a zero vector, i.e., $\boldsymbol{\sigma}' = \langle 0 \quad 0 \quad 0 \quad 0 \rangle^T$.

This was provided by using different constitutive matrices in the stress-strain relations of the beam and the membrane solutions i.e., $\hat{\boldsymbol{\sigma}} = \hat{\mathbf{E}} \hat{\boldsymbol{\varepsilon}}$ (given in section 4) and $\bar{\boldsymbol{\sigma}} = \bar{\mathbf{E}} \bar{\boldsymbol{\varepsilon}}$. Therefore, consideration of the strain field $\boldsymbol{\varepsilon}' = \langle 0 \quad -\nu\varepsilon \quad 0 \quad 0 \rangle^T$ is required only at the boundaries of the local analysis domain, in order to consider the changes in the cross-sectional dimensions while imposing the membrane model boundary conditions. The reason for not including the strains due to Poisson ratio in the beam strain vector is the convenience of the decomposition matrix \mathbf{N} based on the kinematic considerations under rigid sectional contour assumption. At both ends of the membrane model, the displacement vector due to Poisson ratio effect, i.e., $\tilde{\mathbf{d}}_{@i\&j}$ is obtained by numerically integrating the strains, i.e., $-\nu\varepsilon$ over the cross-sectional contour, and then by imposing the condition that the summation of these displacements is zero in order to eliminate the rigid body translations due to $\tilde{\mathbf{d}}_{@i\&j}$. Thus, the displacement boundary conditions imposed onto the membrane model can be written as $\hat{\mathbf{d}}_{@i\&j} \approx \mathbf{N}_{@i\&j} \bar{\mathbf{d}} + \tilde{\mathbf{d}}_{@i\&j}$. In order to separate the membrane internal displacements $\delta \hat{\mathbf{d}}_{IN}$ from the displacement boundary conditions $\tilde{\mathbf{d}}_{@i\&j}$, we can use Eq. (37) to obtain

$$\boxed{\begin{array}{c|c} \hat{\mathbf{K}}_a & \hat{\mathbf{K}}_b \\ \hline \hat{\mathbf{K}}_b^T & \hat{\mathbf{K}}_c \end{array}} \boxed{\begin{array}{c} \delta \hat{\mathbf{d}}_{@i\&j} \\ \delta \hat{\mathbf{d}}_{IN} \end{array}} = \boxed{\begin{array}{c} \delta \hat{\mathbf{f}}_{@i\&j} \\ \delta \hat{\mathbf{f}}_I \end{array}} \quad (38)$$

where $\delta \hat{\mathbf{f}}_I$ denotes the variation of external loads that are applied within the overlapping domain and $\delta \hat{\mathbf{f}}_{@i\&j}$ is the vector of variations in traction forces at the boundaries of the local analysis domain. Specified displacements and load variations for the local membrane analysis are placed in the box symbol (\square).

4. Elasto-plastic constitutive relations of the membrane

The stiffness matrix of the membrane $\hat{\mathbf{K}}$ is updated at each iteration, therefore the algorithmic elasto-plastic tangent modulus $\hat{\mathbf{C}}_{ep}$ is used in its calculation (Simo and Hughes 1998), which is obtained below. When calculating finite increments in the stress, firstly the strain increment based on the last converged strain, i.e., is used in the trial elastic update of the stress, i.e., $\hat{\boldsymbol{\sigma}}^{tr} = \hat{\boldsymbol{\sigma}}_s + \Delta \hat{\boldsymbol{\sigma}}_s^l$, in which $\hat{\boldsymbol{\sigma}}_s$ is the last converged stress and because of the elastic trial assumption, the increment in the stress is calculated as $\Delta \hat{\boldsymbol{\sigma}}_s^l = \hat{\mathbf{E}} \Delta \hat{\boldsymbol{\varepsilon}}_s^l$, in which $\hat{\boldsymbol{\varepsilon}}_s$ is the last converged strain. If the yield condition is satisfied, i.e., $f = \sigma_{ef} - \sigma_{Y0} - H|\lambda| \leq 0$, then $\hat{\boldsymbol{\sigma}}_s^l = \hat{\boldsymbol{\sigma}}^{tr}$, otherwise the trial stress is returned to the yield surface according to the flow rule of the associative plasticity, where σ_{ef} is the effective stress given as $\sigma_{ef} = [\hat{\sigma}_x^2 + \hat{\sigma}_y^2 - \hat{\sigma}_x \hat{\sigma}_y + 3\hat{\tau}_{xy}^2]^{1/2}$, σ_{Y0} is the initial yield stress limit, H is

the hardening modulus and λ is the effective plastic strain. If the trial stress $\hat{\boldsymbol{\sigma}}^{tr}$ is outside the yield surface the Closest-Point Projection algorithm as given in Simo and Hughes (1998) is adopted to impose the flow rule and the consistency condition.

4.1 Elasto-plastic constitutive equations and stress update

The vector of stresses can be written as

$$\hat{\boldsymbol{\sigma}} = \left\langle \hat{\sigma}_x \quad \hat{\sigma}_y \quad \hat{\tau}_{xy} \mid \hat{\tau}_m \right\rangle^T. \quad (39)$$

and the matrix of elastic material properties of the membrane element $\hat{\mathbf{E}}$ can be written as

$$\hat{\mathbf{E}} = \frac{E}{(1-\nu^2)} \begin{bmatrix} 1 & \nu & 0 & \vdots & 0 \\ \nu & 1 & 0 & \vdots & 0 \\ 0 & 0 & \frac{1-\nu}{2} & \vdots & 0 \\ \hline 0 & 0 & 0 & \vdots & \frac{(1-\nu)}{2} \end{bmatrix} \quad (40)$$

in which E is the Young's modulus and ν is the Poisson's ratio. It should be noted that the last diagonal term in Eq. (40) is because of the modification introduced into the potential energy functional. The continuum elasto-plastic stress-strain relations can be written as

$$d\hat{\boldsymbol{\sigma}} = \hat{\mathbf{E}}d\hat{\boldsymbol{\varepsilon}} - d\lambda\hat{\mathbf{E}}\mathbf{a} \quad (41)$$

in which $\mathbf{a} = \partial f / \partial \hat{\boldsymbol{\sigma}}$. The consistency condition during plastic deformation, i.e., $df = 0$ and $d\hat{\boldsymbol{\sigma}} = \hat{\mathbf{E}}(d\hat{\boldsymbol{\varepsilon}} - d\lambda\mathbf{a})$ produces $d\lambda = \mathbf{a}^T \hat{\mathbf{E}} d\hat{\boldsymbol{\varepsilon}} / (\mathbf{a}^T \hat{\mathbf{E}} \mathbf{a} + H)$. After yielding occurs, the flow rule and the consistency condition can be imposed in an incremental iterative procedure. Respectively, the flow rule and the consistency condition can be written in finite incremental form as

$$\mathbf{r} = \Delta\hat{\boldsymbol{\sigma}} - \hat{\mathbf{E}}\Delta\hat{\boldsymbol{\varepsilon}} + \Delta\lambda\hat{\mathbf{E}}\mathbf{a} = 0 \quad (42)$$

$$f(\hat{\boldsymbol{\sigma}}) = 0 \quad (43)$$

The nonlinear set of Eqs. (42) and (43) can be solved according to the Newton-Raphson solution scheme as

$$\begin{bmatrix} \mathbf{I} + \Delta\lambda\hat{\mathbf{E}}\nabla^2 f & \hat{\mathbf{E}}\mathbf{a} \\ \mathbf{a}^T & -H \end{bmatrix} \begin{Bmatrix} \delta\hat{\boldsymbol{\sigma}} \\ \delta\lambda \end{Bmatrix} = - \begin{Bmatrix} \mathbf{r} \\ f \end{Bmatrix} \quad (44)$$

while updating the variables as $\Delta \hat{\boldsymbol{\sigma}}^{j+1} = \Delta \hat{\boldsymbol{\sigma}}^j + \delta \hat{\boldsymbol{\sigma}}^j$ and $\Delta \lambda^{j+1} = \Delta \lambda^j + \delta \lambda^j$ until the conditions $\|\mathbf{r}^j\| < \varepsilon_{tol}$ and $f^j < \varepsilon_{tol}$ are satisfied. In Eq. (44), $\nabla^2 f = \partial^2 f / \partial \hat{\boldsymbol{\sigma}}^2$ and \mathbf{I} is the identity matrix. Upon convergence, the increment in the stress field of the local membrane i.e., $\Delta \hat{\boldsymbol{\sigma}}_s^l$ can be determined and the stress can be updated as $\hat{\boldsymbol{\sigma}}_s^l = \hat{\boldsymbol{\sigma}}_s + \Delta \hat{\boldsymbol{\sigma}}_s^l$. The iterations can be started based on the elastic prediction, i.e., $\Delta \lambda^1 = 0$ and $\Delta \hat{\boldsymbol{\sigma}}^1 = \hat{\mathbf{E}} \Delta \hat{\boldsymbol{\varepsilon}}$. The algorithmic tangent modulus can be defined as the relation $\hat{\mathbf{C}}_{\varphi} = d\Delta \hat{\boldsymbol{\sigma}} / d\Delta \hat{\boldsymbol{\varepsilon}}$. Differentiation of Eq. (42) and multiplying both sides by $\hat{\mathbf{C}}\hat{\mathbf{E}}^{-1}$ produces

$$d\Delta \hat{\boldsymbol{\sigma}} = \hat{\mathbf{C}} d\Delta \hat{\boldsymbol{\varepsilon}} - \hat{\mathbf{C}} a d\Delta \lambda \quad (45)$$

where $\hat{\mathbf{C}} = [\hat{\mathbf{E}}^{-1} + \Delta \lambda \nabla^2 f]^{-1}$. Using the consistency condition, i.e., $df = 0$ in Eq. (45) produces $d\Delta \lambda = \mathbf{a}^T \hat{\mathbf{C}} d\Delta \hat{\boldsymbol{\varepsilon}} / (\mathbf{a}^T \hat{\mathbf{C}} \mathbf{a} + H)$. By substituting $d\Delta \lambda$ into Eq. (45), the algorithmic elasto-plastic tangent modulus according to the current stress update algorithm can be obtained as

$$d\Delta \hat{\boldsymbol{\sigma}} = \hat{\mathbf{C}} d\Delta \hat{\boldsymbol{\varepsilon}} - \hat{\mathbf{C}} a d\Delta \lambda \quad (46)$$

5. Iterative solution procedure

By using Newmark's constant acceleration method (Newmark 1959), and applying it for the global solution, the incremental dynamic equilibrium equation for the current time $t + \Delta t$ can be written as

$$\bar{\mathbf{K}}_{eff\ k} \Delta \bar{\mathbf{d}}_k^n = \Delta \bar{\mathbf{f}}_{eff\ k} + \Delta \bar{\mathbf{R}}_k^n \quad (47)$$

in which the incremental displacement vector $\Delta \bar{\mathbf{d}}_k^n$ is the only unknown quantity, $\bar{\mathbf{K}}_k$ is the effective stiffness matrix of the global analysis at the beginning of the time t corresponding to step k , i.e.,

$$\tilde{\mathbf{K}}_{eff\ k} = \bar{\mathbf{K}}_k + \frac{2}{\Delta t} \bar{\mathbf{C}}_k + \frac{4}{\Delta t^2} \bar{\mathbf{M}}_k, \quad (48)$$

and $\Delta \bar{\mathbf{f}}_{eff\ k}$ is the effective incremental load vector given by

$$\Delta \bar{\mathbf{f}}_{eff\ k} = \Delta \bar{\mathbf{f}}_k + \bar{\mathbf{M}} \left(\frac{4}{\Delta t} \dot{\bar{\mathbf{d}}}_k + 2\ddot{\bar{\mathbf{d}}}_k \right) + 2\bar{\mathbf{C}} \dot{\bar{\mathbf{d}}}_k. \quad (49)$$

In Eq. (47), the increment in the displacement vector $\Delta \bar{\mathbf{d}}_k^n$ is iteratively solved considering the unbalanced force vector $\Delta \bar{\mathbf{R}}_k^n$ calculated from Eq. (28) in each iteration n , i.e.,

$$\Delta \bar{\mathbf{R}}_k^n = \bar{\mathbf{f}}_k - \mathbf{N}^T \int \int_{L A} \hat{\mathbf{B}}_k^{nT} \hat{\mathbf{S}}^T \hat{\boldsymbol{\sigma}}_k^n dA d\bar{z} - \mathbf{N}^T \hat{\mathbf{C}} \hat{\mathbf{d}}_k^n - \mathbf{N}^T \hat{\mathbf{M}} \ddot{\hat{\mathbf{d}}}_k^n \quad (50)$$

The incremental displacement vector $\Delta \bar{\mathbf{d}}_k^n$ can be used to update the displacement $\bar{\mathbf{d}}_k^n = \bar{\mathbf{d}}_k^{n-1} + \Delta \bar{\mathbf{d}}_k^n$, velocity $\dot{\bar{\mathbf{d}}}_k^n = \dot{\bar{\mathbf{d}}}_k^{n-1} + \Delta \dot{\bar{\mathbf{d}}}_k^n$ and acceleration $\ddot{\bar{\mathbf{d}}}_k^n = \ddot{\bar{\mathbf{d}}}_k^{n-1} + \Delta \ddot{\bar{\mathbf{d}}}_k^n$ vectors of the global solution in each iteration n , where

$$\Delta \ddot{\bar{\mathbf{d}}}_k^n = \frac{4}{\delta t^2} \Delta \bar{\mathbf{d}}_k^n - \delta \frac{4}{\delta t} \dot{\bar{\mathbf{d}}}_k^{n-1} - 2\ddot{\bar{\mathbf{d}}}_k^{n-1}, \quad (51)$$

and

$$\Delta \dot{\bar{\mathbf{d}}}_k^n = \frac{2}{\delta t} \Delta \bar{\mathbf{d}}_k^n - 2\dot{\bar{\mathbf{d}}}_k^{n-1}, \quad (52)$$

have been used based on Newmark's constant acceleration method. For the current time $t + \Delta t$, local, displacements and stresses used in Eq. (50) can be updated using the local model in an incremental-iterative manner; firstly, displacement, velocity and acceleration boundary conditions and the load within the global step k , are increasingly imposed in s steps and; secondly, the displacement increments of the internal nodes are determined in l iterations, i.e., $\Delta \hat{\mathbf{d}}_{IN s}^l$, because the unbalanced terms due nonlinearities in the local model, i.e., $\Delta \hat{\mathbf{r}}_{IN s}^l$ should also be corrected in the local model. Thus, from Eq. (38), by using the Newmark's constant acceleration procedure, the local displacement vector of the internal nodes at the l^{th} iteration $\Delta \hat{\mathbf{d}}_{IN s}^l$ can be written as

$$\Delta \hat{\mathbf{d}}_{IN s}^l = \tilde{\mathbf{K}}_{c s}^{-1} \left(\Delta \tilde{\mathbf{f}}_{I s} + \Delta \hat{\mathbf{r}}_{IN s}^l - \hat{\mathbf{K}}_b^T \Delta \hat{\mathbf{d}}_{s @i\&j} - \hat{\mathbf{C}}_b^T \Delta \hat{\mathbf{d}}_{s @i\&j} - \hat{\mathbf{M}}_b^T \Delta \ddot{\hat{\mathbf{d}}}_{s @i\&j} \right) \quad (53)$$

in which $\tilde{\mathbf{K}}_{c s}$ is due to partitioning of the effective stiffness matrix of the local membrane model which is updated in each step s , i.e.,

$$\tilde{\mathbf{K}}_{c s} = \hat{\mathbf{K}}_{c s} + \frac{2}{\Delta t_s} \hat{\mathbf{C}}_c + \frac{4}{\Delta t_s^2} \hat{\mathbf{M}}_c \quad (54)$$

and $\Delta \tilde{\mathbf{f}}_{I s}$ is the due to the portioning of the effective load vector in step s , i.e.,

$$\Delta \tilde{\mathbf{f}}_{I s} = \Delta \hat{\mathbf{f}}_{I s} + \hat{\mathbf{M}}_c \left(\frac{4}{\Delta t_s} \dot{\hat{\mathbf{d}}}_{IN s}^l + 2\ddot{\hat{\mathbf{d}}}_{IN s}^l \right) + 2\hat{\mathbf{C}}_c \hat{\mathbf{d}}_{IN s}^l. \quad (55)$$

The incremental displacement vector $\Delta \hat{\mathbf{d}}_{IN s}^l$ can be used to update the displacement $\hat{\mathbf{d}}_{IN s}^l = \hat{\mathbf{d}}_{IN s}^{l-1} + \Delta \hat{\mathbf{d}}_{IN s}^l$, velocity $\dot{\hat{\mathbf{d}}}_{IN s}^l = \dot{\hat{\mathbf{d}}}_{IN s}^{l-1} + \Delta \dot{\hat{\mathbf{d}}}_{IN s}^l$ and acceleration $\ddot{\hat{\mathbf{d}}}_{IN s}^l = \ddot{\hat{\mathbf{d}}}_{IN s}^{l-1} + \Delta \ddot{\hat{\mathbf{d}}}_{IN s}^l$ vectors of the local solution in each iteration n . It should be noted that the time step Δt_s is in general different from that of the global step, i.e., $\Delta t_s = \Delta t/s$ if the dynamic solution of the local membrane model

is obtained in s steps within the global step k . In Eq. (53), $\Delta \hat{\mathbf{d}}_s @i&j$, $\Delta \hat{\dot{\mathbf{d}}}_s @i&j$ and $\Delta \hat{\ddot{\mathbf{d}}}_s @i&j$ indicate the specified displacement velocity and acceleration increments at the boundaries of the local analysis domain. In Eq. (53), $\Delta \hat{\mathbf{r}}_{IN_s}^l$ is the unbalanced load vector due to the nonlinearities involved in the local membrane problem, which can be obtained from the partitioning of the vector $\Delta \hat{\mathbf{r}}_s^{lT} = \langle \Delta \hat{\mathbf{r}}_{@i&j}^T \mid \Delta \hat{\mathbf{r}}_{IN_s}^{lT} \rangle$ where

$$\Delta \hat{\mathbf{r}}_s^l = \hat{\mathbf{f}}_s - \int \int_{L A} \hat{\mathbf{B}}_s^{lT} \hat{\mathbf{S}}^T \hat{\boldsymbol{\sigma}}_s^l dA d\bar{\Gamma} - \hat{\mathbf{C}} \hat{\mathbf{d}}_s^l - \hat{\mathbf{M}} \hat{\ddot{\mathbf{d}}}_s^l, \quad (56)$$

And $\hat{\mathbf{f}}_s^T = \langle \hat{\mathbf{f}}_{@i&j s}^T \mid \hat{\mathbf{f}}_{I s}^T \rangle$. The incremental nodal displacements obtained from Eq. (53) can be used to update the displacement $\hat{\mathbf{d}}_s^l = \hat{\mathbf{d}}_s^{l-1} + \Delta \hat{\mathbf{d}}_s^l$, velocity $\hat{\dot{\mathbf{d}}}_s^l = \hat{\dot{\mathbf{d}}}_s^{l-1} + \Delta \hat{\dot{\mathbf{d}}}_s^l$ and acceleration $\hat{\ddot{\mathbf{d}}}_s^l = \hat{\ddot{\mathbf{d}}}_s^{l-1} + \Delta \hat{\ddot{\mathbf{d}}}_s^l$ vectors of the local solution in each iteration l , based on which the internal strain field $\hat{\boldsymbol{\epsilon}}_s^l$ can also be updated. Given the strain field $\hat{\boldsymbol{\epsilon}}_s^l$, the details of the update of the stress field $\hat{\boldsymbol{\sigma}}_s^l$ based on elasto-plastic constitutive relations is given in the next section. If the local convergence criterion is satisfied, i.e., $\|\Delta \hat{\mathbf{r}}_s^l\| < \varepsilon_{tol}$ then $\hat{\boldsymbol{\sigma}}_k^n = \hat{\boldsymbol{\sigma}}_s^l$ is used for the calculation of $\Delta \bar{\mathbf{R}}_k^n$ in Eq. (50), within the k^{th} step in the n^{th} iteration. It should be noted that, outside the overlapping region i.e., $\Omega_c \setminus \Omega_m$, where beam solution is deemed accurate, the nodal displacement vector, the internal beam strain field $\bar{\boldsymbol{\epsilon}}_k^n$ and consequently the elastic stress field $\bar{\boldsymbol{\sigma}}_k^n$ can be easily updated from a given $\bar{\mathbf{d}}_k^n$. Thus, outside the overlapping region, $\Delta \bar{\mathbf{R}}_k^n$ in Eq. (50) can be directly calculated without requiring the local membrane solution. The convergence criterion for global equations is deemed satisfied when $\|\Delta \bar{\mathbf{R}}_k^n\| < \varepsilon_{tol}$. Step k is finalized when $\|\Delta \mathbf{V}_k^n\| < \varepsilon_{tol}$ where $\|\Delta \mathbf{V}_k^n\| < \varepsilon_{tol}$ where $\mathbf{V}_k^n = \mathbf{N}^T \int \int_{L A} \hat{\mathbf{B}}_k^{nT} \hat{\mathbf{S}}^T \hat{\boldsymbol{\sigma}}_k^n dA d\bar{\Gamma} + \mathbf{N}^T \hat{\mathbf{C}} \hat{\mathbf{d}}_k^n + \mathbf{N}^T \hat{\mathbf{M}} \hat{\ddot{\mathbf{d}}}_k^n$ and $\Delta \mathbf{V}_k^n = \mathbf{V}_k^n - \mathbf{V}_k^{n-1}$, so that the local and global solutions are synchronized.

6. Case studies

6.1 Simply supported beam under axial and vertical impact loads

The simply supported beam shown in Fig. 2 with a span of 0.6 m, a height of 0.032 m and a thickness of 12 mm is considered for the analysis. The membrane element sizes are $8 \times 8 \text{ mm}^2$. The modulus of elasticity and Poisson ratio are taken as $E=200 \times 10^3 \text{ MPa}$ and $\nu=0.3$, respectively. Density of steel is taken as $7.85 \times 10^{-9} \text{ Nsec}^2/\text{mm}$. It should be noted that in this example the material behaviour is elastic only. The beam is modelled using four beam elements and the overlapping region covers only beam 2 where some elements are missing in the membrane model to represent damage as shown in Fig. 2. Thus, 73 elements are used to model the beam using membrane elements as opposed to 297 elements in the full membrane model as shown in Fig. 2.

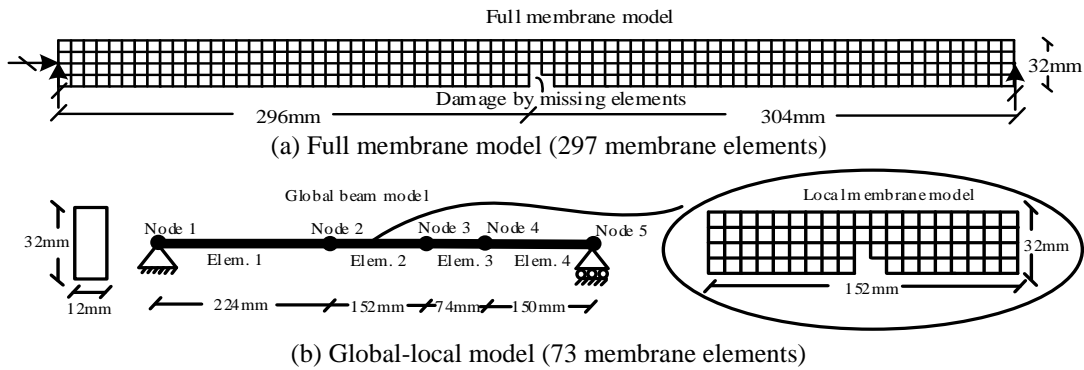


Fig. 2 Model dimensions and boundary conditions in Examples 1 and 2

In both axial and vertical loading cases, the results of the global-local analysis are compared with those of the full membrane analysis for verification purposes as shown in Figs. 3-6. In order to be able to impose the same boundary and loading conditions for membrane and the global-local model throughout the analysis, warping of the cross-section at the ends due to applied loads are prevented by applying Multiple-point constraints at the ends of the membrane model. It should be noted that the same 10^{-5} error tolerance in the Euclid norm of the force vectors is used for convergence check, and the damping constant c is selected as 5×10^{-5} in all cases.

Initially a compressive impact load is applied at the tip (Node 5) of the beam as shown in Fig. 3, and the tip displacement vs. time behaviour is plotted.

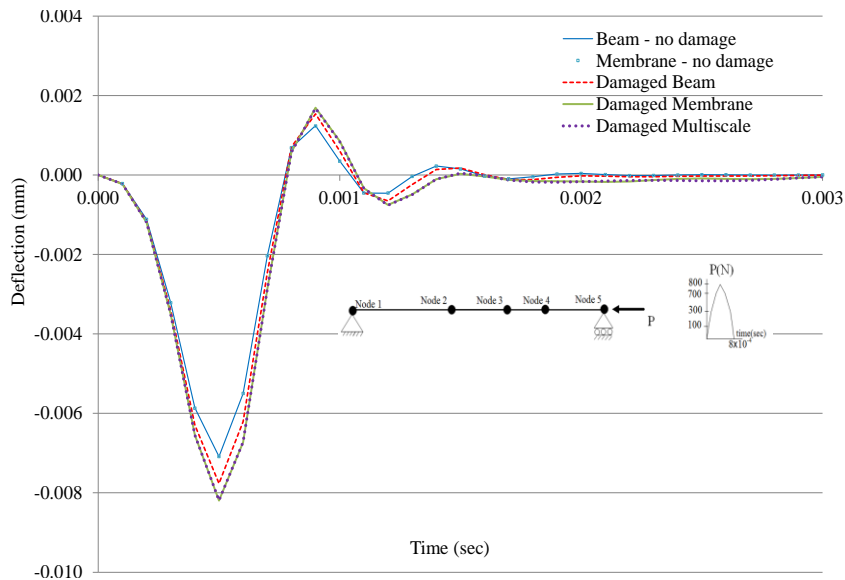


Fig. 3 Axial deflection at the tip vs. time

As shown in Fig. 3, the beam and the membrane solutions fully agree when there is no damage

introduced (i.e., full 300 element membrane model is used) thus, beam solution is very economical. However, the membrane solution and the beam solution do not fully agree when damage is introduced by removing 3 elements at the mid-span of the beam. It should be noted that the beam solution is based on reduced sections used corresponding to the regions where the elements are missing. On the other hand, the global-local analysis is in excellent agreement with the full membrane analysis as shown in Fig. 3 as well as Fig. 4 where the frequency response functions of the displacements are plotted based on the Fast Fourier Transform of the data.

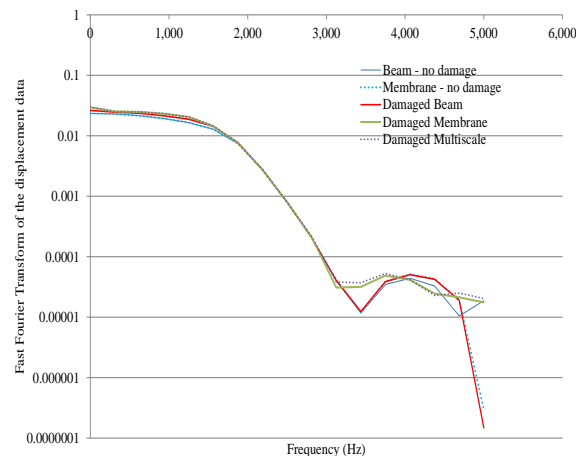


Fig. 4 Fast Fourier Transform of the axial deflection at the tip

In the second case a vertical impact load is applied and the displacement vs. time response is plotted at node 4 as shown in Fig. 5.

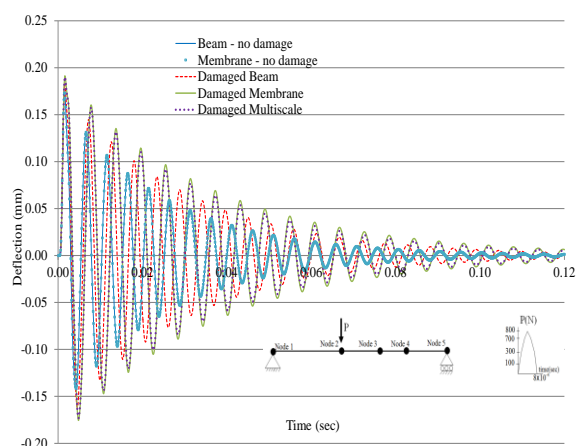


Fig. 5 Vertical deflection vs. time at Node 4

Similar to the first case, the beam and the membrane solutions fully agree when there is no

damage introduced (i.e., full 300 element membrane model is used) thus, beam solution is very economical. However, when damage is introduced by removing 3 elements at the mid-span of the beam the membrane solution and the beam solution do not agree. On the other hand, the global-local analysis is in excellent agreement with the full membrane analysis as shown in Fig. 5 as well as Fig. 6 where the frequency response functions of the displacements are plotted based on the Fast Fourier Transform of the data.

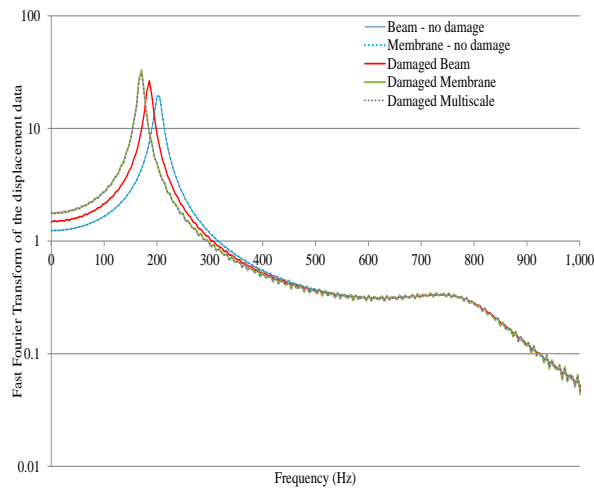


Fig. 6 Fast Fourier Transform of the vertical deflection at Node 4

6.2 Elasto-plastic dynamic analysis of a steel plate shear wall with opening

A cantilever steel plate shear wall with an opening at its base subjected to a cyclic load of $P = 250 \times 10^3 \times \sin(2\pi \times 100t)$ N at its tip is analysed in this section (Fig. 7).

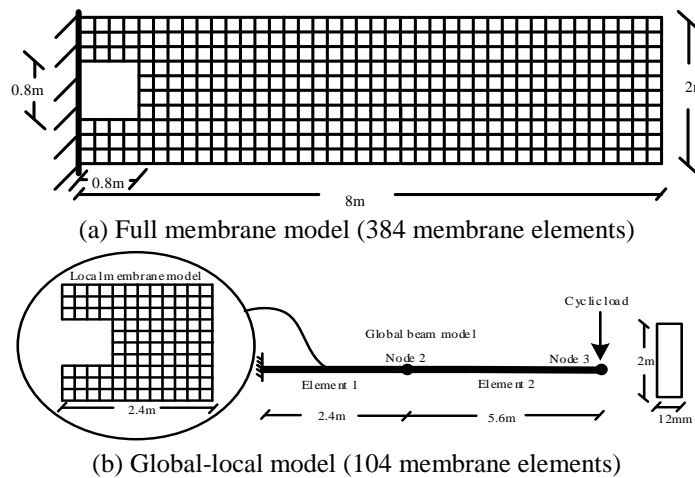


Fig. 7 Model dimensions and boundary conditions in Example 3

The material properties are the same as the previous example, except for the yield limit which is assumed as 260 MPa. The error tolerance and the damping constant c are the same as the previous example. Multiple-point constraints are used at the location of the applied load to prevent warping deformations.

The damage is introduced in terms of an opening in the wall, as is customary in building construction to allow for doors and windows. The analysis is performed using the undamaged and damaged beam, membrane and global-local models. The damaged membrane model is obtained by deleting the elements at the location of the opening while the beam damaged model is created by using reduced section properties in the relative areas to account for the opening.

Neither of the beam solutions reaches the yield limit and therefore the beam analysis remains elastic in both cases. However, plastic deformations occur in the membrane and the global-local analyses. The analysis results are presented in Figs. 8 and 9 in terms of the base moment (the moment at the root of the cantilever) and the displacement at the tip of the beam, respectively. It can be observed that the global-local model has been able to closely capture the effect of the plasticisation with relatively smaller number of elements compared with the membrane model. It is noteworthy to mention that the effect of the localised behaviour on the global response of the element in the regions away from the vicinity of damage (i.e., Fig. 9) is captured accurately without changes in the global model, highlighting the efficiency of the non-intrusive global-local method for that purpose.

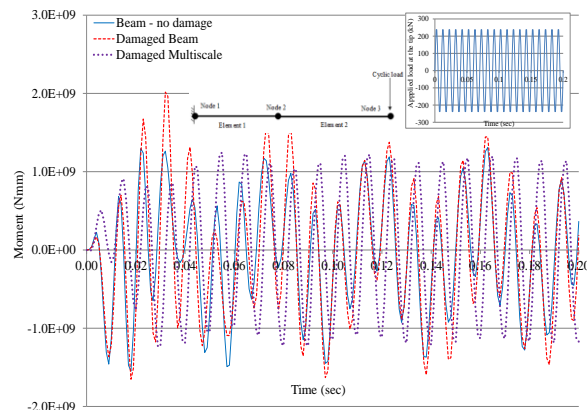


Fig. 8 Base moment at the root of the cantilever

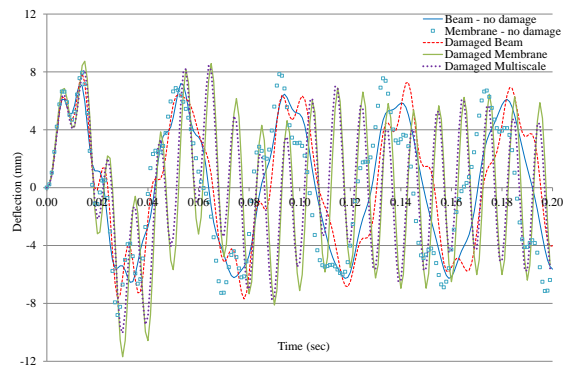


Fig. 9 Tip displacement

7. Conclusions

An iterative global-local method is developed in this study to consider the local effects in the global dynamic behavior of beams. The method implements an overlapping domain decomposition technique to allow the use of beam elements for the global model while adopting sophisticated elasto-plastic membrane elements in the regions where localized deformations are anticipated. Several cases are studied using the developed method and excellent agreement with the full membrane solution is observed. By adopting the proposed method, significant reduction in the number of degrees-of-freedom of the finite element model can be achieved without noticeable compromise in the accuracy of the analysis, which signifies the efficiency of the method in the dynamic analysis of structures with localized nonlinearities.

References

- Allix, O., Gendre, L., Gosselet, P. and Guguin, G. (2011), "Non-intrusive coupling: An attempt to merge industrial and research software capabilities", *Rec. Develop. Innovat. Appl. Comput. Mech.*, **15**, 125-133.
- Afnani, A. and Erkmén, R.E. (2016), "Iterative global-local procedure for the analysis of composite thin-walled laminates", *Steel Compos. Struct.*, **20**, 693-718.
- Babuska, I. and Melenk, J.M. (1995), *The Partition of Unity Finite Element Method (Final Report, Apr. - Jun. 1995)*, Vol. AD-A301760, TN-BN-1185, NIPS-96-41139.
- Banik, S.S., Hong, H.P. and Kopp G.A. (2010), "Assesment of capacity curves for transmission line towers under wind loading", *Wind Struct.*, **13**(1), 1-20.
- Belytschko, T. (2001), "Arbitrary discontinuities in finite elements", *J. Numer. Meth. Eng.*, **50**(4), 993-1013.
- Belytschko, T., Krongauz, Y., Organ, D., Fleming, M. and Krysl, P. (1996), "Meshless methods: An overview and recent developments", *Comput. Meth. Appl. Mech. Eng.*, **139**(1), 3-47.
- Bettinotti, O., Allix, O. and Malherbe, B. (2014), "A coupling strategy for adaptive local refinement in space time with a fixed global model in explicit dynamics", *Comput. Mech.*, **53**, 561-574.
- Bozdogan, K.B. and Ozturk, D. (2016), "A method for dynamic analysis of frame-hinged shear wall structures", *Earthq. Struct.*, **11**(1), 45-61.
- Doyle, J.F. and Farris, T.N. (1995), "Structural mechanics modeling of the impact of a double cantilever beam", *J. Fract.*, **76**(4), 311-326.
- Duarte, C. and Oden, J. (1996), "Hp clouds-an hp meshless method", *Numer. Meth. Part. Differ. Equat.*, **12**, 673-705.
- Duval, M., Passieux, J.C., Salaün, M. and Guinard, S. (2016), "Non-intrusive coupling: Recent advances and scalable nonlinear domain decomposition", *Arch. Comput. Meth. Eng.*, **23**(1), 17-38.
- Erkmén, E. and Bradford, M.A. (2011), "Coupling of finite element and meshfree methods for locking-free analysis of shear-deformable beams and plates", *Eng. Comput.*, **28**(8), 1003-27.
- Erkmén, R. (2013), "Bridging multi-scale approach to consider the effects of local deformations in the analysis of thin-walled members", *Comput. Mech.*, **52**(1), 65-79.
- Erkmén, R.E. (2015), "Multiple-point constraint applications for the finite element analysis of shear deformable composite beams-variational multiscale approach to enforce full composite action", *Comput. Struct.*, **149**, 17-30.
- Erkmén, R.E., Saleh, A. and Afnani, A. (2016), "Incorporating local effects in the predictor step of the iterative global-local analysis of beams", *J. Multisc. Comput. Eng.*, **14**, 455-477.
- Erkmén, R.E. and Saleh, A. (2017), "Iterative global-local approach to consider the effects of local elasto-plastic deformations in the analysis of thin-walled members", *J. Multisc. Comput. Eng.*, **15**, 143-173.
- Erkmén, R.E., Mohareb, M. and Afnani, A. (2017), "Multi-scale overlapping domain decomposition to consider elasto-plastic local buckling effects in the analysis of pipes", *J. Struct. Stab. Dyn.*, **17**, 1-28.

- Farris, T.N. and Doyle, J.F. (1993), "A global/local approach to lengthwise cracked beams-dynamic analysis", *J. Fract.*, **60**(2), 147-156.
- Feyel, F. (2003), "A multilevel finite element method (FE2) to describe the response of highly non-linear structures using generalized continua", *Comput. Meth. Appl. Mech. Eng.*, **192**, 3233-3244.
- Fish, J., Markolefas, S., Guttal, R. and Nayak, P. (1994), "On adaptive multilevel superposition of finite element meshes for linear elastostatics", *Appl. Numer. Math.*, **14**, 135-164.
- Gendre, L., Allix, O., Gosselet, P. and Comte, F. (2009), "Non-intrusive and exact global/local techniques for structural problems with local plasticity", *Comput. Mech.*, **44**(2), 233-245.
- Hadianfard, M.A., Farahani, A. and B-Jahromi, A. (2012), "On the effect of steel column cross-sectional properties on the behaviours when subjected to blast loading", *Struct. Eng. Mech.*, **44**(4), 449-463.
- Hughes, T.J.R., Feijoo, G.R., Mazzei, L. and Quincy, J.B. (1998), "Variational multiscale method-a paradigm for computational mechanics", *Comput. Meth. Appl. Mech. Eng.*, **166**(1), 3-24.
- Hughes, T.J.R. and Sangalli, G. (2007), "Variational multiscale analysis: The fine-scale green's function, projection, optimization, localization, and stabilized methods", *SIAM J. Numer. Anal.*, **45**(2), 539-519.
- Ibrahimbegovic, A., Taylor, R.L. and Wilson, E.L. (1990), "A robust quadrilateral membrane finite element with drilling degrees of freedom", *J. Numer. Meth. Eng.*, **30**(3), 445-457.
- Kerfriden, P., Passieux, J.C. and Bordas, S.P.A. (2012), "Local/global model order reduction strategy for the simulation of quasi-brittle fracture", *J. Numer. Meth. Eng.*, **89**(2), 154-179.
- Knight, N.O.R.M.A.N.F.J.R., Ransom, J., Griffin, O.H.J.R. and Thompson, D. (1991), "Global/local methods research using a common structural analysis framework", *Fin. Elem. Analy. Des.*, **9**, 91-112.
- Lim, H.K., Kang, J.W., Lee, Y.G. and Chi, H.S. (2016), "Seismic performance evaluation of a three-dimensional unsymmetrical reinforced concrete beams", *Multisc. Multiphys. Mech.*, **1**(2), 143-156.
- Liu, W., Hao, S., Belytschko, T., Li, S. and Chang, C. (2000), "Multi-scale methods", *J. Numer. Meth. Eng.*, **50**, 993-1013.
- Mao, K.M. and Sun, C.T. (1991), "A refined global-local finite element analysis method", *J. Numer. Meth. Eng.*, **32**(1), 29-43.
- McConnell, J.R. and Brown, H. (2011), "Evaluation of progressive collapse alternate load path analyses in designing for blast resistance of steel columns", *Eng. Struct.*, **33**(10), 2899-2909.
- Mote, C.D.J.R. (1971), "Global-local finite element (global-local finite element combined ritz methods for beam and plate vibration analysis)", *J. Numer. Meth. Eng.*, **3**, 565-574.
- Newmark, N. (1959), "A method of computational for structural dynamics", *J. Eng. Mech. Div.*, **85**, 67-94.
- Noor, A. (1986), "Global-local methodologies and their application to nonlinear analysis", *Fin. Elem. Analy. Des.*, **2**, 333-346.
- Simo, J.C. and Hughes, T.J.R. (1998), *Computational Inelasticity*, Springer-Verlag (Interdisciplinary Applied Mathematics, New York, U.S.A.
- Strouboulis, T., Copps, K. and Babuska, I. (2001), "The generalized finite element method", *Comput. Meth. Appl. Mech. Eng.*, **190**, 4081-4193.
- Sun, C.T. and Mao, K.M. (1988), "A global-local finite element method suitable for parallel computations", *Comput. Struct.*, **29**(2), 309-315.
- Voleti, S.R., Chandra, N. and Miller, J.R. (1996), "Global-local analysis of large-scale composite structures using finite element method", *Comput. Struct.*, **58**(2), 453-464.
- Whitcomb, J.D. (1991), "Iterative global/local finite element analysis", *Comput. Struct.*, **40**, 1027-1031.
- Whitcomb, J. and Woo, K. (1993a), "Application of iterative global/local finite-element analysis. Part 1: Linear analysis", *J. Numer. Meth. Eng.*, **9**(9), 745-756.
- Whitcomb, J. and Woo, K. (1993b), "Application of iterative global/local finite element analysis. Part 2: Geometrically nonlinear analysis", *J. Numer. Meth. Eng.*, **9**, 757-766.

Appendix

A.1 Interpolation functions of the membrane

The vector of the displacement field shown in Fig. 1(b) can be written as

$$\hat{\mathbf{u}} = \langle \hat{u}_0 \quad \hat{v}_0 \quad \hat{\theta} \rangle^T \tag{A. (1)}$$

which can be interpolated by using nodal displacements as

$$\hat{\mathbf{u}} = \hat{\mathbf{X}}\hat{\mathbf{d}}, \tag{A. (2)}$$

where the nodal displacement vector of an element can be written as

$$\hat{\mathbf{d}} = \langle \hat{u}_1 \quad \hat{v}_1 \quad \hat{\theta}_1 \quad \hat{u}_2 \quad \hat{v}_2 \quad \hat{\theta}_2 \quad \hat{u}_3 \quad \hat{v}_3 \quad \hat{\theta}_3 \quad \hat{u}_4 \quad \hat{v}_4 \quad \hat{\theta}_4 \rangle^T, \tag{A. (3)}$$

and matrix $\hat{\mathbf{X}}$ in Eq. A. (2) can be written as

$$\hat{\mathbf{X}} = \begin{bmatrix} N_1 & 0 & N_1^x & N_2 & 0 & N_2^x & N_3 & 0 & N_3^x & N_4 & 0 & N_4^x \\ 0 & N_1 & N_1^y & 0 & N_2 & N_2^y & 0 & N_3 & N_3^y & 0 & N_4 & N_4^y \\ 0 & 0 & N_1 & 0 & 0 & N_2 & 0 & 0 & N_3 & 0 & 0 & N_4 \end{bmatrix} \tag{A. (4)}$$

in which N_i is the standard bilinear shape function defined as

$$N_i = \frac{1}{4}(1 + \xi_i \xi)(1 + \eta_i \eta), \quad i = 1, 2, 3, 4 \tag{A. (5)}$$

where $\xi = x/a$ and $\eta = y/b$, a and b are the half lengths of the rectangular member in x and y directions respectively. Local coordinates x and y are measured from the middle of the rectangular element, i.e., $-1 \leq \xi \leq 1$ and $-1 \leq \eta \leq 1$. It should also be noted that 2x2 Gaussian quadrature was used for the numerical integration of both plate and membrane. Membrane related functions N_i^x and N_i^y according to Allman-type interpolation are defined as

$$N_i^x = \frac{1}{8}(y_{ij}N_l - y_{ik}N_m), \quad (i = 1, 2, 3, 4) \tag{A. (6)}$$

$$N_i^y = \frac{1}{8}(x_{ij}N_l - x_{ik}N_m), \quad (i = 1, 2, 3, 4) \tag{A. (7)}$$

in which

$$N_m = \frac{1}{2}(1 - \xi^2)(1 + \eta_m \eta), \quad (m = 8, 5, 6, 7) \tag{A. (8)}$$

$$N_l = \frac{1}{2}(1 + \xi_l \xi)(1 - \eta^2), \quad (l = 5, 6, 7, 8). \quad \text{A. (9)}$$

where $x_{ij} = x_j - x_i$, $y_{ij} = y_j - y_i$, $l_{ij}^2 = x_{ij}^2 + y_{ij}^2$, ($ij = 41, 12, 23, 34$) and ($ik = 12, 23, 34, 41$).

A.2 Strains of the membrane element

Strains of the membrane element can be written as

$$\hat{\boldsymbol{\varepsilon}} = \left\langle \hat{\boldsymbol{\varepsilon}}_x \quad \hat{\boldsymbol{\varepsilon}}_y \quad \hat{\gamma}_{xy} \mid \hat{\gamma}_m \right\rangle^T \quad \text{A. (10)}$$

where

$$\hat{\boldsymbol{\varepsilon}} = \left\langle \frac{\partial \hat{u}_0}{\partial x} \quad \frac{\partial \hat{v}_0}{\partial y} \quad \frac{\partial \hat{u}_0}{\partial y} + \frac{\partial \hat{v}_0}{\partial x} \mid \frac{1}{2} \left(\frac{\partial \hat{v}_0}{\partial x} - \frac{\partial \hat{u}_0}{\partial y} \right) - \hat{\theta} \right\rangle^T = \left\langle \begin{array}{c} \hat{\boldsymbol{\varepsilon}}_m \\ \frac{1}{2} \left(\frac{\partial \hat{v}_0}{\partial x} - \frac{\partial \hat{u}_0}{\partial y} \right) - \hat{\theta} \end{array} \right\rangle, \quad \text{A. (11)}$$

in which $\hat{\boldsymbol{\varepsilon}}_m$ is the vector of membrane strains and the last row in Eq. A. (11) contains the skew symmetric part of the membrane strains introduced to avoid numerical stability issues when drilling rotations $\hat{\theta}$ are used with Allman-type interpolations [27].

Matrix $\hat{\mathbf{B}}$ can be written as

$$\hat{\mathbf{B}} = \bar{\mathbf{B}}_m \mathfrak{S} \hat{\mathbf{X}} \quad \text{A. (12)}$$

in which

$$\bar{\mathbf{B}}_m = \begin{bmatrix} 1 & 0 & 0 & 0 & 0 \\ 0 & 1 & 0 & 0 & 0 \\ 0 & 0 & 1 & 1 & 0 \\ 0 & 0 & -\frac{1}{2} & \frac{1}{2} & -1 \end{bmatrix}, \quad \text{A. (13)}$$

$$\mathfrak{S} = \begin{bmatrix} \frac{\partial}{\partial x} & 0 & \frac{\partial}{\partial y} & 0 & 0 \\ 0 & \frac{\partial}{\partial y} & 0 & \frac{\partial}{\partial x} & 0 \\ 0 & 0 & 0 & 0 & 1 \end{bmatrix}^T, \quad \text{A. (14)}$$